
1 **High efficiency of livestock ammonia emission controls on alleviating**
2 **particulate nitrate during a severe winter haze episode in northern China**

3
4 **Zhenying Xu¹, Mingxu Liu¹, Minsi Zhang², Yu Song^{1*}, Shuxiao Wang^{3*}, Lin Zhang⁴,**
5 **Tingting Xu¹, Tiantian Wang¹, Caiqing Yan¹, Tian Zhou¹, Yele Sun⁵, Yuepeng Pan⁵,**
6 **Min Hu¹, Mei Zheng^{1*} and Tong Zhu¹**

7 ¹State Key Joint Laboratory of Environmental Simulation and Pollution Control,
8 Department of Environmental Science, Peking University, Beijing, 100871, China

9 ²National Center for Climate Change Strategy and International Cooperation (NCSC)

10 ³State Key Joint Laboratory of Environment Simulation and Pollution Control, School of
11 Environment, Tsinghua University, Beijing 100084, China

12 ⁴Laboratory for Climate and Ocean-Atmosphere Studies, Department of Atmospheric and
13 Oceanic Sciences, School of Physics, Peking University, Beijing 100871, China

14 ⁵State Key Laboratory of Atmospheric Boundary Layer Physics and Atmospheric
15 Chemistry, Institute of Atmospheric Physics, Chinese Academy of Sciences, Beijing
16 100029, China

17 *Corresponding author: Yu Song (songyu@pku.edu.cn), Shuxiao Wang
18 (shxwang@tsinghua.edu.cn), Mei Zheng (mzheng@pku.edu.cn).

19
20
21
22
23
24
25
26
27
28
29
30

31

32 **Abstract**

33 Although nitrogen oxide (NO_x) emission controls have been implemented for several
34 years, northern China is still facing high particulate nitrate (NO₃⁻) pollution during severe
35 haze events in winter. In this study, the thermodynamic equilibrium model (ISORROPIA-
36 II) and the Weather Research and Forecast model coupled chemistry (WRF-Chem) were
37 used to study the efficiency of NH₃ emission controls on alleviating particulate NO₃⁻ during
38 a severe winter haze episode. We found that particulate NO₃⁻ formation in extremely high
39 pollution is almost NH₃-limited, not NO_x-limited often happened in the other days. The
40 improvements in manure management of livestock husbandry could reduce 40% of total
41 NH₃ emissions (currently 100 kiloton per a month) in winter of northern China.
42 Consequently, particulate NO₃⁻ was reduced by approximately 40% (averagely from 40.8
43 to 25.7 μg/m³). Our results indicate that reducing livestock NH₃ emissions would be highly
44 effective to reduce particulate NO₃⁻ during severe winter haze events.

45

46

47 **1 Introduction**

48 In northern China (including Beijing, Tianjin, Hebei, Shandong, Shanxi and Henan),
49 severe haze pollution events occur frequently during wintertime, with the concentration of
50 PM_{2.5} (particles with an aerodynamic diameter less than 2.5 μm) reaching hundreds of
51 micrograms per cubic meter and SIA (secondary inorganic aerosol) accounting for more
52 than 50% of PM_{2.5} (Zheng et al., 2016; Tan et al., 2018). To mitigate fine particle pollution,
53 the Chinese government has been taking strong measures to control SO₂ emissions
54 (http://www.gov.cn/zwgk/2011-12/20/content_2024895.htm). Since 2007, SO₂ emissions
55 have been reduced by 75% in China (Li et al., 2017). Consequently, the particulate sulfate
56 concentration has also been declining continuously in the past decade (Geng et al., 2017).

57 Although NO_x emissions in 48 Chinese cities decreased by 21% from 2011 to 2015
58 (Liu et al., 2017a), unfortunately, no obvious decreasing trend for particulate NO₃⁻ had been
59 observed in northern China during recent years (Zhang et al., 2015). In October 2015, a
60 severe haze episode was reported in North China Plain (NCP), with the hourly peak
61 concentration of particulate NO₃⁻ exceeding 70 μg/m³ (Zhang et al., 2018b). Even in
62 November 2018, during a heavy haze episode in northern China, the hourly peak
63 concentration of PM_{2.5} still exceeded 289 μg/m³, of which particulate NO₃⁻ accounted for
64 30% (http://www.mee.gov.cn/xxgk2018/xxgk/xxgk15/201811/t20181116_674022.html).

65 Another way to alleviate the particulate NO₃⁻ pollution is to control NH₃ emissions.
66 Previous studies were performed to demonstrate the necessity of NH₃ emissions abatement
67 in reducing PM_{2.5} concentrations in the United States (Pinder et al., 2007; Tsimpidi et al.,
68 2007; Pinder et al., 2008; Wu et al., 2016) and Europe (de Meij et al., 2009; Bessagnet et al.,
69 2014; Backes et al., 2016). Recently, a feature article pointed out that NH₃ could be key to
70 limiting particulate pollution (Plautz, 2018). In contrast with low particulate matter
71 pollution levels in the United States and Europe, what we are facing in northern China is
72 the extremely high particulate NO₃⁻ pollution especially happened in severe winter haze

73 events.

74 Although Fu et al. (2017) proposed that the NH₃ emission controls are urgently
75 required in China, the effectiveness of NH₃ emissions mitigation to alleviate the particulate
76 NO₃⁻ peaks during severe winter haze episodes was seldom reported. Only Guo et al.
77 (2018b) used a thermodynamic model to estimate the sensitivity of particulate NO₃⁻ to TA
78 (sum of ammonia and ammonium) during one winter haze episode in Beijing. In their study,
79 the atmospheric chemistry simulations based on NH₃ emission controls scenario were
80 lacking to demonstrate the regional effects.

81 To alleviate severe particulate NO₃⁻ pollution in northern China is urgent, the study on
82 the effectiveness by NH₃ emission controls is necessary. In this study, we firstly compile a
83 comprehensive NH₃ emission inventory for northern China in winter of 2015, and estimate
84 the NH₃ emission reductions by improving manure management. Then, the ISORROPIA-
85 II and WRF-Chem models are used to investigate the effectiveness of NH₃ emission
86 reductions on alleviating particulate NO₃⁻ during a severe haze episode. The molar ratio
87 based on observations is used to explore the efficiency of particulate NO₃⁻ reductions
88 during the severe haze conditions in wintertime.

89

90 **2 Methods and Materials**

91 **2.1 Observational data**

92 Hourly time-resolution aerosol and gas measurements were conducted at the Peking
93 University urban atmosphere environment monitoring station (PKUERS) (39.991N,
94 116.313E) in Beijing in December 2015 and December 2016. A commercialized semi-
95 continuous In-situ Gas and Aerosol Composition (IGAC) Monitor was used to measure the
96 concentrations of water-soluble ions (e.g., NH₄⁺, SO₄²⁻, NO₃⁻, Na⁺, K⁺, Ca²⁺, Mg²⁺, Cl⁻) in
97 PM_{2.5} and inorganic gases (e.g., NH₃, HNO₃, HCl). Relative humidity (RH) and
98 temperature were observed at 1-min resolution at the same site. The quality assurance and
99 control for the IGAC was described in Liu et al. (2017b). A typical severe haze episode
100 occurred during the 6 to 10 in December 2015, with daily average concentrations of PM_{2.5}
101 exceeding 150 µg/m³ for three days (PM_{2.5} data are from China National Environmental
102 Monitoring Centre). The average RH and temperature in this haze event were 60.9 ± 11.4%
103 and 276.5 ± 1.4 K. The south wind was dominant with wind speed mostly less than 3 m/s.
104 The average concentrations of particulate NO₃⁻, NH₄⁺ and SO₄²⁻ were 39.8 ± 14.7 µg/m³,
105 27.7 ± 8.6 µg/m³ and 42.4 ± 16.0 µg/m³, respectively. The ratios of particulate NO₃⁻
106 concentrations to SNA (including sulfate, nitrate and ammonium) were 36.5 ± 4.0%.

107 **2.2 NH₃ emission inventory**

108 A comprehensive NH₃ emission inventory of northern China (including the six
109 provinces mentioned above) in December 2015 at a monthly and 1 km × 1 km resolution
110 is developed based our previous studies (Huang et al., 2012;Kang et al., 2016). Here is a
111 brief introduction to our inventory. More detailed descriptions and validation are in our
112 previous studies. Our NH₃ emission inventory is a bottom-up process-based and statistical
113 model which considers a diverse range of sources, including both agricultural (livestock
114 manure and chemical fertilizer) and non-agricultural sectors (e.g., traffic, biomass burning
115 etc.). According to our inventory, the estimated NH₃ emission amount in northern China

116 was 100 kiloton in December 2015. The largest source was livestock waste (57 kiloton,
117 57.0% of the total emissions), following by vehicle (12.2%), chemical industry (8.8%),
118 biomass burning (5.4%), waste disposal (4.0%), synthetic fertilizer applications (2.4%) and
119 other minor sources (9.1%). The proportion of chemical fertilizer is small due to the limited
120 fertilization activity in winter. In the past few years, our inventory has been compared with
121 many studies to prove its reliability. For example, the spatial pattern of NH_3 emissions
122 calculated in our inventory agreed well with the distribution of the NH_3 column
123 concentrations in eastern Asia retrieved from the satellite measurements of Infrared
124 Atmospheric Sounding Interferometer (IASI) (Van Damme et al., 2014). Specially, our
125 estimation of livestock NH_3 emissions in China is comparable to the results of Streets et al.
126 (2003) and Ohara et al. (2007).

127 Another method for estimating NH_3 emissions is the inverse modeling method, which
128 provides top-down emission estimates through optimizing comparisons of model
129 simulations with measurements. For example, Paulot et al. (2014) used the adjoint of a
130 global chemical transport model (GEOS-Chem) and data of NH_4^+ wet deposition fluxes to
131 optimize NH_3 emissions estimation in China. Zhang et al. (2018a) applied TES satellite
132 observations of NH_3 column concentration and GEOS-Chem to provide top-down
133 constraints on NH_3 emissions in China. Their estimates are 10.2 Tg a^{-1} and 11.7 Tg a^{-1}
134 respectively, which are close to our results (9.8 Tg a^{-1}) (Paulot et al., 2014; Zhang et al.,
135 2018a). The accuracy of this method relies on many factors, such as the accuracy of initial
136 conditions, the emission inventories, meteorological inputs, reaction rate constants, and
137 deposition parameters in the chemical transport model. Errors of these parameters could
138 cause biases in the top-down estimation of NH_3 emissions. In addition, measurements of
139 NH_3 or NH_4^+ used in this method, including surface and satellite data, are usually sparse in
140 spatial coverage and have uncertainties, which will also affect the estimation of NH_3
141 emissions.

142 2.3 ISORROPIA-II and WRF-Chem models

143 The thermodynamic equilibrium model, ISORROPIA-II (Fountoukis and Nenes,
144 2007), being used to determine the phase state and composition of an NH_4^+ - SO_4^{2-} - NO_3^- -
145 K^+ - Ca^{2+} - Mg^{2+} - Na^+ - Cl^- - H_2O aerosol system with its corresponding gas components
146 in thermodynamic equilibrium, was used to investigate the response of particulate NO_3^- to
147 NH_3 emission reductions. Using measurements of water-soluble ions, T and RH from
148 PKUERS as inputs, ISORROPIA-II can avoid the inherent uncertainty in estimates of
149 emission inventories, pollutant transport, and chemical transformation. In this study,
150 ISORROPIA-II was run in the “forward mode” and assuming particles are “metastable”
151 with no solid precipitates, which is due to the relatively high RH range observed during
152 this haze event ($\text{RH} = 60.9 \pm 11.4\%$).

153 We assess the performance of ISORROPIA-II by comparing measured and predicted
154 particulate NO_3^- , NH_4^+ and gaseous HNO_3 , NH_3 . An error metric, the mean bias (MB), is
155 used to quantify the bias (the description of MB is shown below Figure S1). The predicted
156 particulate NO_3^- , NH_4^+ and NH_3 agree well with the measurements and the value of R^2 are
157 0.99, 0.94 and 0.84, respectively (Figure S1). The MB is only $1.0 \mu\text{g}/\text{m}^3$, $0.3 \mu\text{g}/\text{m}^3$ and -
158 $1.8 \mu\text{g}/\text{m}^3$, respectively. However, the model performs poorly on HNO_3 , with an R^2 of only
159 0.06 and a MB of $-1.0 \mu\text{g}/\text{m}^3$. This is because particulate NO_3^- is predominantly in the
160 particle phase (the mass ratio of particulate NO_3^- to the total nitric acid ($\text{TN} = \text{NO}_3^- + \text{HNO}_3$))

161 was $99.2 \pm 1.9\%$), small errors in predicting particulate NO_3^- are amplified in HNO_3
162 predicting. Since the MB of HNO_3 is much smaller than the observed particulate NO_3^- (39.8
163 $\pm 14.7 \mu\text{g}/\text{m}^3$) and NH_4^+ ($27.7 \pm 8.6 \mu\text{g}/\text{m}^3$), this bias have little influence on simulating the
164 efficiency of particulate NO_3^- reductions.

165 In the real atmosphere, changes in the level of TA ($\text{TA} = \text{NH}_4^+ + \text{NH}_3$) can affect the
166 lifetime of TN (Pandis and Seinfeld, 1990). This is because the gaseous HNO_3 has a faster
167 deposition rate in the atmosphere than particulate NO_3^- , and reductions in NH_4^+ may
168 prompt particulate NO_3^- partitioning into the gas phase. In such a case, the concentration
169 of TN would not remain constant but decrease. In order to consider these, we use the
170 Weather Research and Forecast Model coupled Chemistry (WRF-Chem) model (ver. 3.6.1)
171 to investigate the effect of NH_3 emission controls on particulate NO_3^- formation in the
172 regional scale. The simulations were performed for the severe haze event during 6 to 10
173 December 2015. The modeling domain covered the whole northern China with horizontal
174 resolution of 25 km and 24 vertical layers from surface to 50 hPa. The initial meteorological
175 fields and boundary conditions were taken from the 6 h National Centers for Environmental
176 Prediction (NCEP) global final analysis with a $1^\circ \times 1^\circ$ spatial resolution. The inorganic
177 gas-aerosol equilibrium was predicted by Multicomponent Equilibrium Solver for Aerosols
178 (MESA) in WRF-Chem (Zaveri et al., 2005). The Carbon-Bond Mechanism version Z
179 (CBMZ) photochemical mechanism and Model for Simulating Aerosol Interactions and
180 Chemistry (MOSAIC) aerosol model were used in this study (Fast et al., 2006).
181 Anthropogenic emissions from power plants, industrial sites, residential locations, and
182 vehicles were taken from the Multi-resolution Emission Inventory for China (MEIC;
183 available at www.meicmodel.org).

184 The performance of WRF-Chem is evaluated by comparing measured and simulated
185 NO_3^- , NH_4^+ , SO_4^{2-} and TA. Specifically, the observed and simulated values are, respectively:
186 (1) NO_3^- , $39.8 \pm 14.7 \mu\text{g}/\text{m}^3$ versus $39.1 \pm 15.6 \mu\text{g}/\text{m}^3$; (2) NH_4^+ , $27.7 \pm 8.6 \mu\text{g}/\text{m}^3$ versus
187 $26.5 \pm 11.7 \mu\text{g}/\text{m}^3$; (3) SO_4^{2-} , $42.4 \pm 16.0 \mu\text{g}/\text{m}^3$ versus $39.7 \pm 20.8 \mu\text{g}/\text{m}^3$ and (4) TA, 34.6
188 $\pm 8.5 \mu\text{g}/\text{m}^3$ versus $32.1 \pm 11.0 \mu\text{g}/\text{m}^3$. The MB of these four species are -0.7, -1.2, -2.7 and
189 $-2.5 \mu\text{g}/\text{m}^3$, respectively. Simulated particulate NO_3^- , NH_4^+ , SO_4^{2-} and TA approximately
190 agreed with the measurements (Figure S2). There are still some simulation biases that may
191 affect the simulation of particulate NO_3^- reductions efficiency. This is discussed in detail
192 in Sect 3.3.

193

194 **3 Results**

195 **3.1 High potential reduction of wintertime NH_3 emissions in northern China**

196 Livestock husbandry accounts for the largest proportion of NH_3 emissions in winter of
197 northern China (approximately 60%), which is mainly caused by the poor manure
198 management. There are three main animal-rearing systems in China: free-range, grazing
199 and intensive. On the one hand, the proportion of intensive livestock husbandry in China
200 is only about 40%, far lower than that of developed countries (Harun and Ogneva-
201 Himmelberger., 2013). As a result, the widespread free-range and grazing animal rearing
202 systems contribute more than half of the total livestock NH_3 emissions due to lacking
203 manure collection and treatment (Kang et al., 2016). On the other hand, there were no
204 relevant regulations about storage of manure for intensive farms in China in the past few

205 decades. This causes most livestock farms also lack necessary measures and facilities for
206 manure collection and storage (Chadwick et al., 2015).

207 Due to the current poor manure management in China, the improved manure
208 management may have great potential for NH₃ emission reductions from livestock
209 husbandry (Wang et al., 2017). The improved manure management mainly includes three
210 phases: in-house handling, storage and land application (Chadwick et al., 2011). For winter,
211 the emission reduction measures mainly focus on in-house handling and storage, since land
212 application mainly occurs in spring and summer. According to previous studies, for in-
213 house handling, regularly washing the floor and using slatted floor or deep litter to replace
214 solid floor could both reduce NH₃ emissions by more than 50% (Groenestein and
215 VanFaassen, 1996; Monteny and Erisman, 1998; Gilhespy et al., 2009; Hou et al., 2015). For
216 storage, covering slurry and manure could reduce NH₃ emissions by about 50%-70%
217 (Balsari. et al., 2006; Petersen et al., 2013; Hou et al., 2015; Wang et al., 2017).

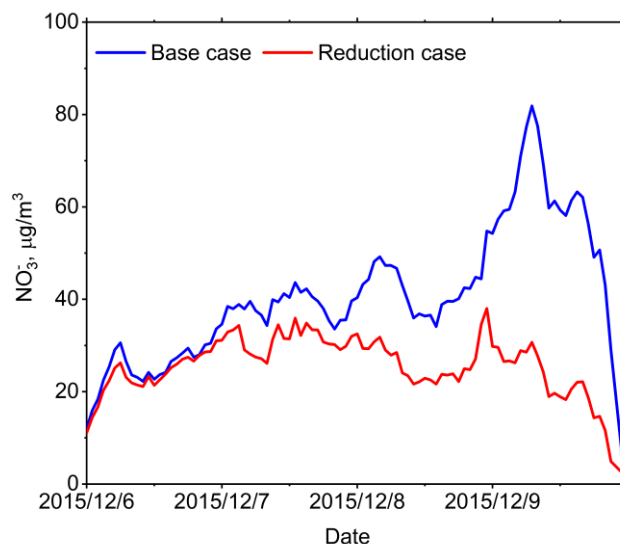
218 Based on the above research results, the livestock NH₃ emission reductions strategies
219 applied in this study include the following steps. Firstly, the proportion of intensive
220 livestock production was raised from 40% to 80% in our NH₃ emission inventory model.
221 In our model, the animals in free-range and grazing animal rearing systems are assumed to
222 live outdoors for half a day, and the improved manure management is only effective for
223 indoor animals. Therefore, increasing the proportion of intensive livestock production is
224 conducive to better manure management (Hristov et al., 2011). Secondly, the ratios of NH₃
225 emission reductions mentioned above were multiplied by NH₃ emission factors in two
226 phases of manure management: 50% reduction at in-house handling and 60% (average
227 value of 50% and 70%) reduction at storage. With these measures, we estimate that the
228 NH₃ emission factors for the livestock in China could be comparable to those in Europe
229 and the USA (shown in Table S1). Meanwhile, our NH₃ emission model predicted that the
230 livestock NH₃ emissions were reduced by 60% (from 57 to 23 kiloton), causing
231 approximately 40% reduction in total NH₃ emissions. Spatially, NH₃ emissions decreased
232 significantly in Hebei, Henan and Shandong, where the livestock NH₃ emissions accounted
233 for a large proportion of the total (shown in Figure S3).

234 **3.2. Simulations of NO₃⁻ reduction due to NH₃ emission controls**

235 In the ISORROPIA-II simulation, 40% reduction of TA was used to reflect the effects
236 of reducing NH₃ emissions by 40%. This approach has been used in many previous studies
237 (Blanchard and Hidy, 2003; Vayenas et al., 2005). However, in the real atmosphere, the
238 reductions of NH₃ emission are not always equal to the reductions of TA due to the regional
239 transmission. Their differences are discussed in the WRF-Chem simulation.

240 In this haze event (from 6 to 10 December, 2015), the mean concentration of particulate
241 NO₃⁻ decreased from 40.8 to 25.7 μg/m³ (a 37% reduction). In addition, the peak hourly
242 concentration of NO₃⁻ decreased from 81.9 to 30.7 μg/m³ (a 63% reduction) (shown in
243 Figure 1). The fundamental thermodynamic processes of TA reductions on decreasing
244 particulate NO₃⁻ are explained below. Firstly, we found that NH₃ was quite available to
245 react with HNO₃ in the thermodynamic equilibrium system, because NH₃ was 6.6 ± 3.8
246 μg/m³ while HNO₃ was only 0.4 ± 1.1 μg/m³. Secondly, almost all of particulate NO₃⁻
247 condensed into aerosol phase (the mass ratio of particulate NO₃⁻ to TN was 99.2 ± 1.9%)
248 under such low temperature conditions (276.5 ± 1.4 K). Thirdly, the NH₃-HNO₃ partial

249 pressure production (K_p) was as low as about 0.1 ppb² (calculated from ISORROPIA-II
250 outputs, depending not only on temperature and RH but also sulfate concentration). The
251 value of K_p would remain constant, if the temperature, RH and sulfate concentration
252 remained unchanged. In general, NH_4NO_3 was not easy to volatilize into gas phase under
253 these circumstances.



254

255 **Figure 1.** A comparison of particulate nitrate (NO_3^-) between the base (blue line) and
256 emission reductions cases (red line) simulated by the ISORROPIA-II model in this severe
257 haze episode.

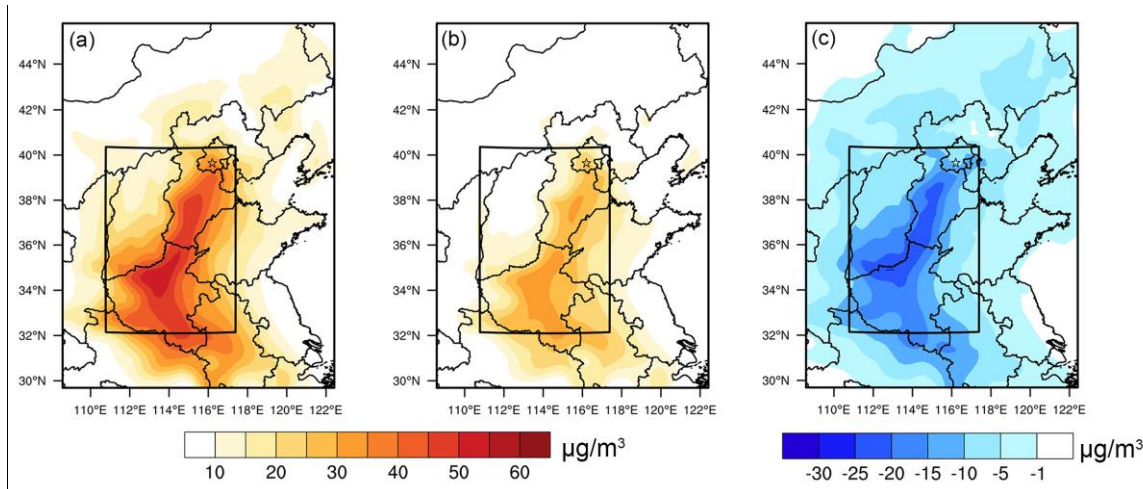
258

259 When TA was reduced by 40%, the average mass concentration of gaseous NH_3
260 decreased from 6.6 to 0.01 $\mu\text{g}/\text{m}^3$ (from 8.8 ppb to 0.05 ppb). In order to keep the value of
261 K_p constant in the thermodynamic equilibrium state, the reductions of NH_3 increased HNO_3 ,
262 which shifted the particulate NO_3^- partitioning toward the gas phase. Hence, when NH_3 in
263 gas phase was almost completely depleted, HNO_3 increased from 0.4 to 15.5 $\mu\text{g}/\text{m}^3$ (from
264 0.1 ppb to 5.6 ppb), leading to a reduction of particulate NO_3^- from 40.8 to 25.7 $\mu\text{g}/\text{m}^3$ (a
265 37.0 % reduction). Meanwhile, NH_4^+ also decreased from 27.9 to 20.6 $\mu\text{g}/\text{m}^3$ and there was
266 almost no change in sulfate level (decreased from 39.7 to 39.3 $\mu\text{g}/\text{m}^3$), with only trace
267 amount of NH_4HSO_4 produced. This indicated that the reduction of particulate NH_4^+ and
268 NO_3^- was mainly due to the reduction of NH_4NO_3 . The sum of particulate NO_3^- and NH_4^+
269 decreased from 68.7 to 46.3 $\mu\text{g}/\text{m}^3$ (a 32.6% reduction).

270

271 We also conducted WRF-Chem simulations to quantify the impacts of NH_3 emission
272 controls on particulate NO_3^- regionally. A 60% reduction in livestock NH_3 emissions was
273 used as an emission reductions scheme and Figure 2 shows the spatial distribution of
274 particulate NO_3^- under the base case and the emission reductions case. The spatial
275 distribution of particulate NO_3^- was mainly concentrated in most parts of Henan (HN) and
276 Hebei (HB), with the average concentration over 30 $\mu\text{g}/\text{m}^3$ (included in the black box
277 shown in Figure 2a). The highest particulate NO_3^- concentrations, more than 60 $\mu\text{g}/\text{m}^3$,
were mainly located in central south of Hebei and northern Henan. In the emission

278 reductions case, the mean concentration of particulate NO_3^- decreased from 30.6 to 18.5
 279 $\mu\text{g}/\text{m}^3$ (a 39.4% reduction) in the range of the black box. Meanwhile, the particulate NH_4^+
 280 decreased from 16.3 to 11.7 $\mu\text{g}/\text{m}^3$ (a 28.1% reduction). The sum of particulate NO_3^- and
 281 NH_4^+ decreased from 46.9 to 30.2 $\mu\text{g}/\text{m}^3$ (a 35.6% reduction). Besides, the sulfate
 282 concentration slightly changed from 19.7 to 17.6 $\mu\text{g}/\text{m}^3$, and $\text{PM}_{2.5}$ concentration dropped
 283 from 143.4 to 125.4 $\mu\text{g}/\text{m}^3$. The largest reductions in particulate NO_3^- were mainly located
 284 in the central north of Henan and central Hebei, where the percentage reduction was
 285 generally more than 60% (shown in Figure 2b). In some areas with high particulate NO_3^-
 286 concentrations, particulate NO_3^- had been effectively reduced by more than 30 $\mu\text{g}/\text{m}^3$
 287 (shown in Figure 2c). In these regions, severe haze events occurred frequently due to their
 288 large emissions of air pollutants, including NH_3 (Wang et al., 2014; Zhao et al., 2017). In
 289 addition, TN was reduced by 34.1% (from 31.8 $\mu\text{g}/\text{m}^3$ to 21.0 $\mu\text{g}/\text{m}^3$), which was in line
 290 with the assumption in Sect 2.3. Correspondingly, TA decreased by 40.7% (from 17.2
 291 $\mu\text{g}/\text{m}^3$ to 10.2 $\mu\text{g}/\text{m}^3$), very close to the reductions of NH_3 emission (40%). This indicates
 292 that it is reasonable to use TA reductions to represent NH_3 emission reductions in the
 293 ISORROPIA-II simulation.



294

295 **Figure 2.** Spatial distribution of particulate NO_3^- concentrations in northern China
 296 predicted by WRF-Chem from 6 to 10 December, 2015, for (a) the base case, (b) the
 297 emission reductions case and (c) the difference between the base case and the emission
 298 reductions case. The scope of this study focuses on the black box, including Beijing (BJ),
 299 Tianjin (TJ), Hebei (HB), Shanxi (SX), Shandong (SD) and Henan (HN).

300

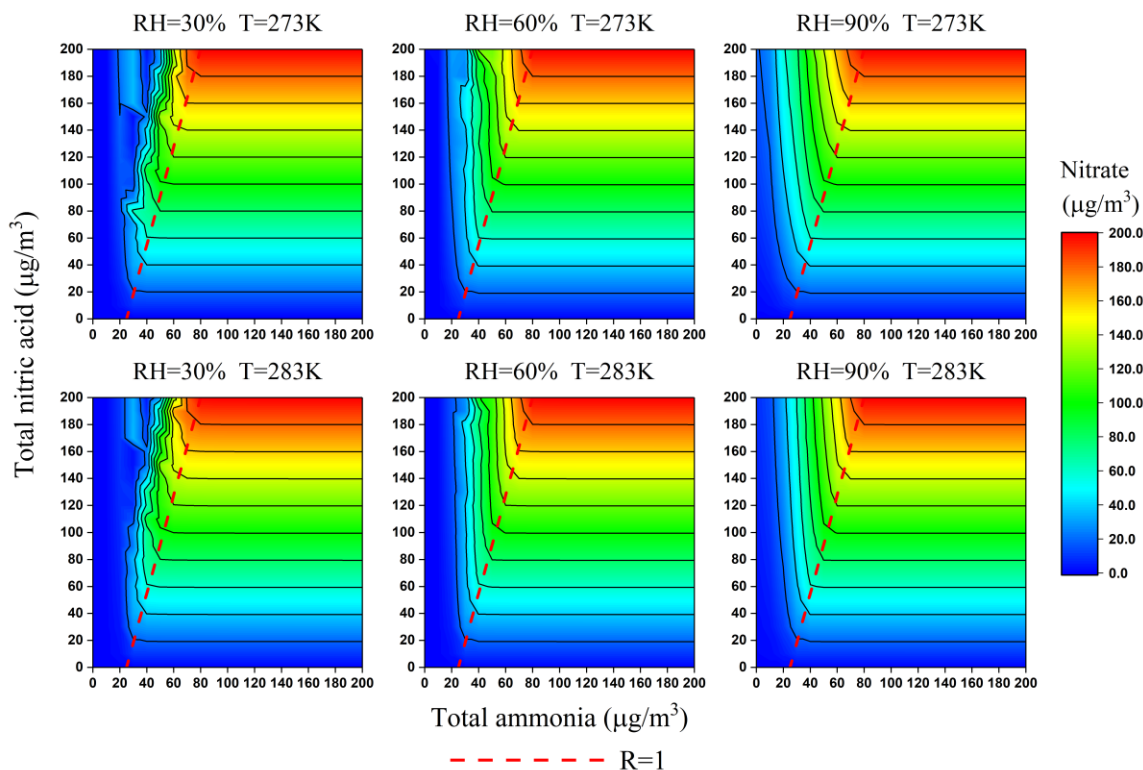
301 3.3 The particulate NO_3^- reduction efficiency during the wintertime

302 The sensitivity of particulate NO_3^- to NH_3 is often determined by the availability of
 303 ambient NH_3 , which can be represented by the observable indicator (Seinfeld and Pandis,
 304 2006). In this study, we use the observed molar ratio (R) of TA to the sum of sulfate, total
 305 chlorine and TN minus Na^+ , K^+ , Ca^{2+} and Mg^{2+} to represent the availability of ambient
 306 NH_3 and predict the sensitivity of the particulate NO_3^- to changes in TN and TA.

307

$$R = \frac{TA}{2SO_4^{2-} + NO_3^- + HNO_3(g) + Cl^- + HCl(g) - 2Ca^{2+} - Na^+ - K^+ - 2Mg^{2+}} \quad (1)$$

308 The accuracy of R was examined by constructing the isopleths of particulate NO_3^-
 309 concentrations as a function of TN and TA (shown in Figure 3). The NO_3^- concentration
 310 was constructed by varying the input concentrations of TA and TN from 0 to $200 \mu\text{g}/\text{m}^3$
 311 in increments of $10 \mu\text{g}/\text{m}^3$ independently in ISORROPIA-II, while using the observed average
 312 value for the other components. Over a range of temperatures (273–283 K) and RHs (30–
 313 90%), the dashed line of $R = 1$ divides each isopleth into two regions with tiny bias, which
 314 indicates that R can be used to qualitatively predict the response of the particulate NO_3^- to
 315 changes in concentrations of TN and TA.



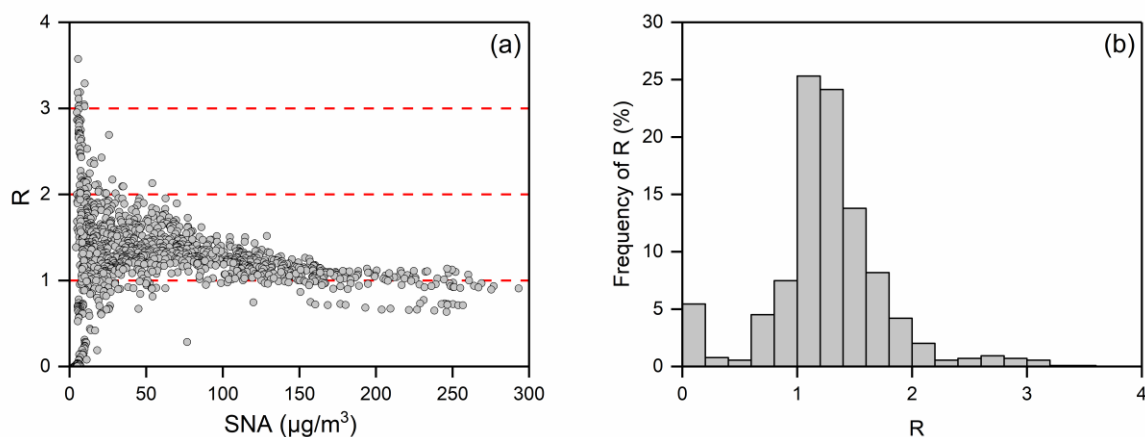
316

317 **Figure 3.** Isopleths of the particulate NO_3^- concentration ($\mu\text{g}/\text{m}^3$) as a function of TN and
 318 TA under average severe haze conditions in winter. The concentration of SO_4^{2-} , Cl^- , K^+ ,
 319 Ca^{2+} , Na^+ , and Mg^{2+} was 60.2, 9.3, 0.56, 0.04, 0.75, and 0.03 $\mu\text{g}/\text{m}^3$, respectively. Values
 320 are averages from all severe hazes during the observation period.

321

322 In the right side of the dashed line ($R > 1$), particulate NO_3^- formation is HNO_3 -limited.
 323 The NH_3 is surplus and almost all particulate NO_3^- exists in the aerosol phase. The TA
 324 reductions mainly reduce NH_3 , with negligible effects on particulate NO_3^- . By contrast,
 325 particulate NO_3^- formation is NH_3 -limited in the left of the dashed line ($R < 1$). There is
 326 less NH_3 present in the gas phase, and TA reductions could reduce particulate NO_3^-
 327 efficiently. For example, when the concentrations of TN and TA are 100 and $50 \mu\text{g}/\text{m}^3$ (RH
 328 = 60 % and $T = 273 \text{ K}$), the concentration of particulate NO_3^- is about $100 \mu\text{g}/\text{m}^3$ and the
 329 value of R is close to one (typical observational values during the severe haze in this study).
 330 In such cases, if TA were reduced by 50% to $25 \mu\text{g}/\text{m}^3$, the particulate NO_3^- would be
 331 significantly reduced from 100 to $20 \mu\text{g}/\text{m}^3$, an 80% reduction.

332 Under the typical winter conditions in northern China, the value of R was generally
333 greater than one and gradually declining with the increase in SNA concentrations (shown
334 in Figure 4a). When the concentration of SNA is greater than $150 \mu\text{g}/\text{m}^3$, the values of R
335 become close to and frequently lower than one. This indicated that particulate NO_3^-
336 formation would easily become NH_3 -limited under severe haze conditions when NH_3
337 emissions were reduced. In general, particulate NO_3^- will be reduced effectively by a 40%
338 reduction of NH_3 emissions in the condition that the value of R is less than 1.4 (shown in
339 Figure S4). This situation accounts for 68.1% of the entire December (shown in Figure 4b).
340 It should also be noted that the particulate NO_3^- is insensitive to a 40% reduction in NH_3
341 emissions when the value of R is greater than 1.4 (shown in Figure S4). This situation
342 mainly occurs in relatively clean days (the concentration of SNA is less than $75 \mu\text{g}/\text{m}^3$),
343 accounting for only 31.9% of the entire December (shown in Figure 4a and 4b). Overall,
344 reducing 40% of NH_3 emissions could effectively reduce the levels of particulate NO_3^-
345 under typical severe winter haze conditions in northern China.



346
347 **Figure 4.** (a) The observed molar ratio (R) and the concentrations of SNA in PKUERS in
348 December 2015 and December 2016. (b) The frequency of R during the same period.

349
350 The observed R provides a simple method to rapidly estimate the efficiency of NH_3
351 emission reductions on the particulate NO_3^- reductions, which can avoid the shortage of the
352 air quality model, especially the uncertain estimates of meteorology. However, it also needs
353 to be examined in more detail for specific pollution and meteorological conditions.
354 Therefore, the observed indicator and air quality models should be used in a
355 complementary way to assess the effectiveness of NH_3 emission controls strategies.

356 Based on the above analysis, the influence of WRF-Chem simulation biases on
357 particulate NO_3^- reduction efficiency simulation mainly depends on the simulation bias of
358 R. During the simulation case, the average simulated value of R is 1.3, which is equivalent
359 to the observed value (1.3). Since WRF-Chem has a good estimation of the availability of
360 ambient NH_3 , its estimation of the efficiency of particulate NO_3^- reductions is reliable.

361 It is noteworthy that the efficiency of particulate NO_3^- reductions by NH_3 emission
362 controls in northern China during severe winter hazes may be higher than that in the United
363 States and Europe. Compared with our results (40% NH_3 emission reductions lead to about

364 40% particulate NO₃⁻ reductions), in the United States and Europe, NH₃ emissions often
365 need to be reduced by more than 70% before particulate NO₃⁻ begin to decrease (Poizzer et
366 al., 2017;Guo et al., 2018a). This is mainly because the strict emission controls of SO₂ and
367 NO_x in these areas lead to a more ammonia-rich environment, which makes particulate
368 NO₃⁻ insensitive to NH₃ emission reductions.

369

370 **4 Conclusions**

371 In this study, we found that during severe winter haze episodes, the particulate NO₃⁻
372 formation is NH₃-limited, resulting in its high sensitivity to NH₃ emission reductions.
373 Meanwhile, livestock NH₃ emission controls is a very efficient way to alleviate particulate
374 NO₃⁻ pollution during severe winter hazes. The estimations showed that the improvements
375 in manure management of livestock husbandry could effectively reduce total NH₃
376 emissions by 40% (from 100 kiloton to 60 kiloton) in winter of northern China. It would
377 lead to a reduction of particulate NO₃⁻ by about 40% (averagely from 40.8 to 25.7 μg/m³)
378 during severe haze conditions.

379 NO_x emission controls could be a more direct and effective way to reduce the
380 particulate NO₃⁻ than NH₃ emission reductions. However, in northern China, the target of
381 NO_x emission reductions is only about 25% in the 13th Five-Year Plan (2016-2020)
382 (http://www.gov.cn/zhengce/content/2017-01/05/content_5156789.htm). Due to the
383 dominance of free-range animal rearing systems and the lack of emission controls policies,
384 livestock NH₃ emission reductions in China could be practicable. In order to control PM_{2.5}
385 pollution more effectively in northern China, measures to improve manure management in
386 livestock urgently need to be implemented.

387

388 **Author contribution**

389 Y.S, S.W and M.Z initiated the investigation. C.Y, T.Z and M.Z conducted the aerosol
390 and gas measurements. Z.X, T.W and M.L performed the modelling analyses. Z.X, S.W,
391 L.Z, C.Y and M.Z wrote and edited the manuscript. M.Z, T.X, T.W, Y.S, Y.P, M.H and T.Z
392 contributed to discussions of the results and the manuscript.

393

394 **Acknowledgement**

395 This study was funded by the National Key R&D Program of China
396 (2016YFC0201505), National Natural Science Foundation of China (NSFC) (91644212
397 and 41675142) and National Research Program for Key Issues in Air Pollution Control
398 (DQGG0208). The model input data and the NH₃ emission inventory used in this study are
399 available from the corresponding author. The authors declare no competing interests.

400

401 **References**

402

403 Backes, A. M., Aulinger, A., Bieser, J., Matthias, V., and Quante, M.: Ammonia emissions
404 in Europe, part II: How ammonia emission abatement strategies affect secondary
405 aerosols, *Atmos. Environ.*, 126, 153-161, 10.1016/j.atmosenv.2015.11.039, 2016.

406 Balsari, P., Dinuccio, E., and Gioelli, F.: A low cost solution for ammonia emission
407 abatement from slurry storage, *International Congress Series*,
408 10.1016/j.ics.2006.02.045, 2006.

409 Bessagnet, B., Beauchamp, M., Guerreiro, C., de Leeuw, F., Tsyro, S., Colette, A., Meleux,
410 F., Rouil, L., Ruysenaars, P., Sauter, F., Velders, G. J. M., Foltescu, V. L., and van
411 Aardenne, J.: Can further mitigation of ammonia emissions reduce exceedances of
412 particulate matter air quality standards?, *Environ Sci Policy*, 44, 149-163,
413 10.1016/j.envsci.2014.07.011, 2014.

414 Blanchard, C. L., and Hidy, G. M.: Effects of changes in sulfate, ammonia, and nitric acid
415 on particulate nitrate concentrations in the southeastern United States, *J Air Waste
416 Manage*, 53, 283-290, Doi 10.1080/10473289.2003.10466152, 2003.

417 Chadwick, D., Sommer, S. G., Thorman, R., Fanguero, D., Cardenas, L., Amon, B., and
418 Misselbrook, T.: Manure management: Implications for greenhouse gas emissions,
419 *Anim Feed Sci Tech*, 166-67, 514-531, 10.1016/j.anifeedsci.2011.04.036, 2011.

420 Chadwick, D., Jia, W., Tong, Y. A., Yu, G. H., Shen, Q. R., and Chen, Q.: Improving
421 manure nutrient management towards sustainable agricultural intensification in
422 China, *Agr Ecosyst Environ*, 209, 34-46, 10.1016/j.agee.2015.03.025, 2015.

423 de Meij, A., Thunis, P., Bessagnet, B., and Cuvelier, C.: The sensitivity of the CHIMERE
424 model to emissions reduction scenarios on air quality in Northern Italy, *Atmos.
425 Environ.*, 43, 1897-1907, 10.1016/j.atmosenv.2008.12.036, 2009.

426 Fast, J. D., Gustafson, W. I., Easter, R. C., Zaveri, R. A., Barnard, J. C., Chapman, E. G.,
427 Grell, G. A., and Peckham, S. E.: Evolution of ozone, particulates, and aerosol direct
428 radiative forcing in the vicinity of Houston using a fully coupled meteorology-
429 chemistry-aerosol model, *J. Geophys. Res.-Atmos.*, 111, 10.1029/2005jd006721,
430 2006.

431 Fountoukis, C., and Nenes, A.: ISORROPIA II: a computationally efficient
432 thermodynamic equilibrium model for K^+ - Ca^{2+} - Mg^{2+} - NH_4^+ - Na^+ - SO_4^{2-} - NO_3^- - Cl^- -
433 H_2O aerosols, *Atmos. Chem. Phys.*, 7, 4639-4659, 10.5194/acp-7-4639-2007, 2007.

434 Fu, X., Wang, S. X., Xing, J., Zhang, X. Y., Wang, T., and Hao, J. M.: Increasing Ammonia
435 Concentrations Reduce the Effectiveness of Particle Pollution Control Achieved via
436 SO_2 and NO_x Emissions Reduction in East China, *Environ. Sci. Technol. Lett.*, 4,
437 221-227, 2017.

438 Geng, G., Zhang, Q., Tong, D., Li, M., Zheng, Y., Wang, S., and He, K.: Chemical
439 composition of ambient $PM_{2.5}$ over China and relationship to precursor emissions
440 during 2005–2012, *Atmos. Chem. Phys.*, 17, 9187-9203, 10.5194/acp-17-9187-2017,
441 2017.

442 Gilhespy, S. L., Webb, J., Chadwick, D. R., Misselbrook, T. H., Kay, R., Camp, V., Retter,
443 A. L., and Bason, A.: Will additional straw bedding in buildings housing cattle and
444 pigs reduce ammonia emissions?, *Biosyst Eng*, 102, 180-189,
445 10.1016/j.biosystemseng.2008.10.005, 2009.

446 Groenestein, C. M., and VanFaassen, H. G.: Volatilization of ammonia, nitrous oxide and
447 nitric oxide in deep-litter systems for fattening pigs, *J Agr Eng Res*, 65, 269-274,
448 DOI 10.1006/jaer.1996.0100, 1996.

449 Guo, H., Otjes, R., Schlag, P., Kiendler-Scharr, A., Nenes, A., and Weber, R. J.:
450 Effectiveness of Ammonia Reduction on Control of Fine Particle Nitrate,
451 Atmospheric Chemistry and Physics Discussions, 1-31, 10.5194/acp-2018-378,
452 2018a.

453 Guo, H. Y., Otjes, R., Schlag, P., Kiendler-Scharr, A., Nenes, A., and Weber, R. J.:
454 Effectiveness of ammonia reduction on control of fine particle nitrate, *Atmos Chem*
455 *Phys*, 18, 12241-12256, 10.5194/acp-18-12241-2018, 2018b.

456 Harun, S. M. R., and Ogneva-Himmelberger., Y.: Distribution of Industrial Farms in the
457 United States and Socioeconomic, Health, and Environmental Characteristics of
458 Counties, *Geography Journal*, org/10.1155/2013/385893, 2013.

459 Hou, Y., Velthof, G. L., and Oenema, O.: Mitigation of ammonia, nitrous oxide and
460 methane emissions from manure management chains: a meta-analysis and integrated
461 assessment, *Glob. Change Biol.*, 21, 1293-1312, 2015.

462 Hristov, A. N., Hanigan, M., Cole, A., Todd, R., McAllister, T. A., Ndegwa, P. M., and
463 Rotz, A.: Review: Ammonia emissions from dairy farms and beef feedlots, *Can J*
464 *Anim Sci*, 91, 1-35, 2011.

465 Huang, X., Song, Y., Li, M. M., Li, J. F., Huo, Q., Cai, X. H., Zhu, T., Hu, M., and Zhang,
466 H. S.: A high-resolution ammonia emission inventory in China, *Glob. Biogeochem.*
467 *Cycle*, 26, 10.1029/2011gb004161, 2012.

468 Kang, Y. N., Liu, M. X., Song, Y., Huang, X., Yao, H., Cai, X. H., Zhang, H. S., Kang, L.,
469 Liu, X. J., Yan, X. Y., He, H., Zhang, Q., Shao, M., and Zhu, T.: High-resolution
470 ammonia emissions inventories in China from 1980 to 2012, *Atmos. Chem. Phys.*,
471 16, 2043-2058, 10.5194/acp-16-2043-2016, 2016.

472 Li, C., McLinden, C., Fioletov, V., Krotkov, N., Carn, S., Joiner, J., Streets, D., He, H.,
473 Ren, X., Li, Z., and Dickerson, R. R.: India Is Overtaking China as the World's
474 Largest Emitter of Anthropogenic Sulfur Dioxide, *Sci Rep*, 7, 14304,
475 10.1038/s41598-017-14639-8, 2017.

476 Liu, F., Beirle, S., Zhang, Q., van der, A. R., Zheng, B., Tong, D., and He, K.: NOx
477 emission trends over Chinese cities estimated from OMI observations during 2005 to
478 2015, *Atmos Chem Phys*, 17, 9261-9275, 10.5194/acp-17-9261-2017, 2017a.

479 Liu, M. X., Song, Y., Zhou, T., Xu, Z. Y., Yan, C. Q., Zheng, M., Wu, Z. J., Hu, M., Wu,
480 Y. S., and Zhu, T.: Fine particle pH during severe haze episodes in northern China,
481 *Geophys. Res. Lett.*, 44, 5213-5221, 10.1002/2017gl073210, 2017b.

482 Monteny, G. J., and Erisman, J. W.: Ammonia emission from dairy cow buildings: A
483 review of measurement techniques, influencing factors and possibilities for reduction,
484 *Neth J Agr Sci*, 46, 225-247, 1998.

485 Ohara, T., Akimoto, H., Kurokawa, J., Horii, N., Yamaji, K., Yan, X., and Hayasaka, T.:
486 An Asian emission inventory of anthropogenic emission sources for the period 1980-
487 2020, *Atmos. Chem. Phys.*, 7, 4419-4444, DOI 10.5194/acp-7-4419-2007, 2007.

488 Pandis, S. N., and Seinfeld, J. H.: On the Interaction between Equilibration Processes and
489 Wet or Dry Deposition, *Atmos Environ a-Gen*, 24, 2313-2327, 10.1016/0960-
490 1686(90)90325-H, 1990.

491 Paulot, F., Jacob, D. J., Pinder, R. W., Bash, J. O., Travis, K., and Henze, D. K.: Ammonia
492 emissions in the United States, European Union, and China derived by high-
493 resolution inversion of ammonium wet deposition data: Interpretation with a new

494 agricultural emissions inventory (MASAGE_NH₃), *J. Geophys. Res.-Atmos.*, 119,
495 4343-4364, 10.1002/2013jd021130, 2014.

496 Petersen, S. O., Dorno, N., Lindholm, S., Feilberg, A., and Eriksen, J.: Emissions of CH₄,
497 N₂O, NH₃ and odorants from pig slurry during winter and summer storage, *Nutr Cycl*
498 *Agroecosys*, 95, 103-113, 10.1007/s10705-013-9551-3, 2013.

499 Pinder, R. W., Adams, P. J., and Pandis, S. N.: Ammonia emission controls as a cost-
500 effective strategy for reducing atmospheric particulate matter in the eastern United
501 States, *Environ. Sci. Technol.*, 41, 380-386, 10.1021/es060379a, 2007.

502 Pinder, R. W., Gilliland, A. B., and Dennis, R. L.: Environmental impact of atmospheric
503 NH₃ emissions under present and future conditions in the eastern United States,
504 *Geophys. Res. Lett.*, 35, Artn L1280810.1029/2008gl033732, 2008.

505 Plautz, J.: Piercing the Haze, *Science*, 361, 1060-1063, 10.1126/science.361.6407.1060,
506 2018.

507 Pozzer, A., Tsimpidi, A. P., Karydis, V. A., de Meij, A., and Lelieveld, J.: Impact of
508 agricultural emission reductions on fine-particulate matter and public health, *Atmos.*
509 *Chem. Phys.*, 17, 12813-12826, 10.5194/acp-17-12813-2017, 2017.

510 Seinfeld, J. H., and Pandis, S. N.: *Atmospheric chemistry and physics : from air pollution*
511 *to climate change*, 2nd ed., Wiley, New York, xxviii, 1202 p. pp., 2006.

512 Streets, D. G., Bond, T. C., Carmichael, G. R., Fernandes, S. D., Fu, Q., He, D., Klimont,
513 Z., Nelson, S. M., Tsai, N. Y., Wang, M. Q., Woo, J. H., and Yarber, K. F.: An
514 inventory of gaseous and primary aerosol emissions in Asia in the year 2000, *J.*
515 *Geophys. Res.-Atmos.*, 108, Artn 880910.1029/2002jd003093, 2003.

516 Tan, T. Y., Hu, M., Li, M. R., Guo, Q. F., Wu, Y. S., Fang, X., Gu, F. T., Wang, Y., and
517 Wu, Z. J.: New insight into PM_{2.5} pollution patterns in Beijing based on one-year
518 measurement of chemical compositions, *Sci. Total Environ.*, 621, 734-743,
519 10.1016/j.scitotenv.2017.11.208, 2018.

520 Tsimpidi, A. P., Karydis, V. A., and Pandis, S. N.: Response of inorganic fine particulate
521 matter to emission changes of sulfur dioxide and ammonia: The eastern United States
522 as a case study, *J Air Waste Manage*, 57, 1489-1498, 10.3155/1047-3289.57.12.1489,
523 2007.

524 Van Damme, M., Clarisse, L., Heald, C. L., Hurtmans, D., Ngadi, Y., Clerbaux, C., Dolman,
525 A. J., Erisman, J. W., and Coheur, P. F.: Global distributions, time series and error
526 characterization of atmospheric ammonia (NH₃) from IASI satellite observations,
527 *Atmos. Chem. Phys.*, 14, 2905-2922, 10.5194/acp-14-2905-2014, 2014.

528 Vayenas, D. V., Takahama, S., Davidson, C. I., and Pandis, S. N.: Simulation of the
529 thermodynamics and removal processes in the sulfate-ammonia-nitric acid system
530 during winter: Implications for PM_{2.5} control strategies, *J. Geophys. Res.-Atmos.*,
531 110, Artn D07s1410.1029/2004jd005038, 2005.

532 Wang, L. T., Wei, Z., Yang, J., Zhang, Y., Zhang, F. F., Su, J., Meng, C. C., and Zhang,
533 Q.: The 2013 severe haze over southern Hebei, China: model evaluation, source
534 apportionment, and policy implications, *Atmos. Chem. Phys.*, 14, 3151-3173,
535 10.5194/acp-14-3151-2014, 2014.

536 Wang, Y., Dong, H. M., Zhu, Z. P., Gerber, P. J., Xin, H. W., Smith, P., Opio, C., Steinfeld,
537 H., and Chadwick, D.: Mitigating Greenhouse Gas and Ammonia Emissions from
538 Swine Manure Management: A System Analysis, *Environ. Sci. Technol.*, 51, 4503-
539 4511, 2017.

540 Wu, Y. Y., Gu, B. J., Erisman, J. W., Reis, S., Fang, Y. Y., Lu, X. H., and Zhang, X. M.:
541 PM_{2.5} pollution is substantially affected by ammonia emissions in China, *Environ.*
542 *Pollut.*, 218, 86-94, 10.1016/j.envpol.2016.08.027, 2016.

543 Zaveri, R. A., Easter, R. C., and Peters, L. K.: A computationally efficient multicomponent
544 equilibrium solver for aerosols (MESA), *J. Geophys. Res.-Atmos.*, 110,
545 10.1029/2004jd005618, 2005.

546 Zhang, L., Chen, Y. F., Zhao, Y. H., Henze, D. K., Zhu, L. Y., Song, Y., Paulot, F., Liu,
547 X. J., Pan, Y. P., Lin, Y., and Huang, B. X.: Agricultural ammonia emissions in China:
548 reconciling bottom-up and top-down estimates, *Atmos. Chem. Phys.*, 18, 339-355,
549 10.5194/acp-18-339-2018, 2018a.

550 Zhang, R., Sun, X. S., Shi, A. J., Huang, Y. H., Yan, J., Nie, T., Yan, X., and Li, X.:
551 Secondary inorganic aerosols formation during haze episodes at an urban site in
552 Beijing, China, *Atmos. Environ.*, 177, 275-282, 10.1016/j.atmosenv.2017.12.031,
553 2018b.

554 Zhang, X. Y., Wang, J. Z., Wang, Y. Q., Liu, H. L., Sun, J. Y., and Zhang, Y. M.: Changes
555 in chemical components of aerosol particles in different haze regions in China from
556 2006 to 2013 and contribution of meteorological factors, *Atmos. Chem. Phys.*, 15,
557 12935-12952, 10.5194/acp-15-12935-2015, 2015.

558 Zhao, B., Wu, W. J., Wang, S. X., Xing, J., Chang, X., Liou, K. N., Jiang, J. H., Gu, Y.,
559 Jang, C., Fu, J. S., Zhu, Y., Wang, J. D., Lin, Y., and Hao, J. M.: A modeling study
560 of the nonlinear response of fine particles to air pollutant emissions in the Beijing-
561 Tianjin-Hebei region, *Atmos. Chem. Phys.*, 17, 12031-12050, 10.5194/acp-17-
562 12031-2017, 2017.

563 Zheng, G. J., Duan, F. K., Ma, Y. L., Zhang, Q., Huang, T., Kimoto, T., Cheng, Y. F., Su,
564 H., and He, K. B.: Episode-Based Evolution Pattern Analysis of Haze Pollution:
565 Method Development and Results from Beijing, China, *Environ. Sci. Technol.*, 50,
566 4632-4641, 10.1021/acs.est.5b05593, 2016.

567